

Video Article

A Mouse Model for Laser-induced Choroidal Neovascularization

Ronil S. Shah¹, Brian T. Soetikno¹, Michelle Lajko¹, Amani A. Fawzi¹

¹Department of Ophthalmology, Northwestern University Feinberg School of Medicine

Correspondence to: Amani A. Fawzi at amani.fawzi@northwestern.edu

URL: <https://www.jove.com/video/53502>

DOI: [doi:10.3791/53502](https://doi.org/10.3791/53502)

Keywords: Medicine, Issue 106, Laser-induced choroidal neovascularization, experimental CNV, age-related macular degeneration, neovascular age-related macular degeneration, wet AMD

Date Published: 12/27/2015

Citation: Shah, R.S., Soetikno, B.T., Lajko, M., Fawzi, A.A. A Mouse Model for Laser-induced Choroidal Neovascularization. *J. Vis. Exp.* (106), e53502, doi:10.3791/53502 (2015).

Abstract

The mouse laser-induced choroidal neovascularization (CNV) model has been a crucial mainstay model for neovascular age-related macular degeneration (AMD) research. By administering targeted laser injury to the RPE and Bruch's membrane, the procedure induces angiogenesis, modeling the hallmark pathology observed in neovascular AMD.

First developed in non-human primates, the laser-induced CNV model has come to be implemented into many other species, the most recent of which being the mouse. Mouse experiments are advantageously more cost-effective, experiments can be executed on a much faster timeline, and they allow the use of various transgenic models. The miniature size of the mouse eye, however, poses a particular challenge when performing the procedure. Manipulation of the eye to visualize the retina requires practice of fine dexterity skills as well as simultaneous hand-eye-foot coordination to operate the laser. However, once mastered, the model can be applied to study many aspects of neovascular AMD such as molecular mechanisms, the effect of genetic manipulations, and drug treatment effects.

The laser-induced CNV model, though useful, is not a perfect model of the disease. The wild-type mouse eye is otherwise healthy, and the chorio-retinal environment does not mimic the pathologic changes in human AMD. Furthermore, injury-induced angiogenesis does not reflect the same pathways as angiogenesis occurring in an age-related and chronic disease state as in AMD.

Despite its shortcomings, the laser-induced CNV model is one of the best methods currently available to study the debilitating pathology of neovascular AMD. Its implementation has led to a deeper understanding of the pathogenesis of AMD, as well as contributing to the development of many of the AMD therapies currently available.

Video Link

The video component of this article can be found at <https://www.jove.com/video/53502/>

Introduction

Age-related macular degeneration (AMD) is one of the leading causes of blindness in individuals over the age of 50¹⁻³. AMD can be classified into two forms: atrophic ("dry") AMD and neovascular ("wet") AMD. The former is characterized by geographic atrophy of the retinal pigment epithelium (RPE), choriocapillaris, and photoreceptors, while the latter is characterized by the invasion of abnormal vessels from the choroid into the outer retinal layers causing leakage, hemorrhage, and fibrosis, and ultimately leading to blindness^{1,2}. Of the two forms, neovascular AMD accounts for the majority of vision loss¹. Fortunately, this form has numerous effective pharmacological management options, whereas its atrophic counterpart currently has no proven medical treatments³. Moreover, because the neovascular form has been easily re-capitulated in an animal model, it has been more widely accessible to basic AMD research exploring the underlying pathological mechanisms in order to develop novel therapies⁴.

The first animal model of experimental choroidal neovascularization (CNV) was developed by Ryan *et al.* in non-human primates⁵. This model induced rupture of Bruch's membrane via laser photocoagulation, which caused a local inflammatory response resulting in angiogenesis similar to that seen in neovascular AMD. The histopathological progression of angiogenesis post-laser induction was found to mimic neovascular AMD, which confirmed the model's validity⁶. Non-human primates offer the most similar anatomy to humans, but unfortunately, are expensive to maintain, cannot be easily genetically manipulated, and have a slow time course of disease progression⁷. Contrastingly, rodent models are much more cost-effective to maintain, can be genetically manipulated with relative ease, and have a much faster course of disease progression (experiments can be conducted on a time scale of weeks versus months). These experiments should only be conducted in pigmented rodents as it is very difficult to visualize in albino animals.

The mouse laser-induced CNV model, first developed by the Campochiaro group in the late 90's¹⁰, has grown to be the dominant animal model in the majority of recent studies¹¹⁻¹⁶. Due to the complex and still unclear pathogenesis of CNV, the laser model has been applied in all aspects of wet AMD research ranging from studying the molecular mechanisms driving angiogenesis to evaluating new treatment modalities for future human use. For example, Sakurai *et al.* and Espinosa-Heidmann *et al.* used the laser model to investigate the effect of macrophages

on the development of CNV using transgenic mice and pharmacological depletion treatments^{15, 16}. Giani *et al.* and Hoerster *et al.* used optical-coherence tomography (OCT) to image the laser-induced CNV in an effort to characterize the progression of CNV and compare the histopathologic findings to the findings seen on OCT imaging^{12, 17}. Finally, studies involving intravitreal injection of anti-angiogenic agents have been used as pre-requisites for human trials and were vital in developing the first generation of anti-VEGF agents used in management of neovascular AMD today^{10, 18, 19}.

Alternative models for experimental CNV utilize surgical methods to induce CNV. This procedure involves injecting pro-angiogenic substances (e.g. recombinant viral vectors overexpressing VEGF, subretinal injection of RPE cells and/or polystyrene beads) to mimic the increased VEGF expression seen in neovascular AMD, with the goal of causing angiogenesis^{8, 20}. However, this method yields a drastically lower incidence of neovascularization; these studies showed that CNV in C57/BL6 mice occurs in 31% of injections versus the ~70% success rate seen in the laser photocoagulation method in the same strain of mice^{8, 14}. For these reasons, and given the advantages of using rodents versus non-human primates, the mouse model of laser-induced CNV has become the standard animal model of CNV for most neovascular AMD study experiments⁸.

The mouse eye is a miniscule, delicate tissue to work with. Maneuvering of the eye to visualize the retina is difficult and requires much practice until mastery is achieved. This task is complicated by the fact that it must be learned with the dominant and non-dominant hand. Furthermore, after the fine movements required to visualize the retina have been learned, the coordination between both hands and the foot pedal operating the laser are important. In this paper, we sought to distill the challenges of learning all of the physical manipulations involved in the laser-induced CNV procedure into a guide that would help operators achieve rapid success with this model.

Protocol

All animals are treated in accordance with the Guide of the Care and Use of Laboratory Animals 2013 Edition, the Association for Research in Vision and Ophthalmology (ARVO) Statement for the Use of Animals in Ophthalmic and Vision Research, and as approved by the Institutional Animal Care and Use Committee for Northwestern University.

Note: The following procedure can be done entirely with one operator; however, it is much more efficiently conducted with two operators with the tasks split accordingly.

1. Prepare Laser and Pre-laser Station

- Position the laser and slit lamp where it can be easily accessible. Turn on laser and set to pre-determined parameters (e.g. 75 μ m spot size, 100 mW power, 100 msec duration).
CAUTION: Ensure operator wears all animal and laser safety personal protective equipment and pertinent laser safety signs are displayed outside of the procedure room.
 - Before using any experimental animals, find ideal parameters using a calibration, non-experimental mouse. Laser parameters will depend on the laser used. Ideal parameters are defined by the lowest laser power setting that consistently causes "bubble" formation when properly focused. See video for example of lesion with proper "bubble" formation.
- Prepare the pre-laser station so that anesthesia, animal warmer, tissue wipes, and all eye drops (Tropicamide, Tetracaine, and artificial tears) are easily within reach to operator.
 - Ensure that animal warmer is pre-heated to correct temperature (37 °C) before injecting anesthetic into first mouse in order to avoid anesthesia-induced hypothermia.
- Place mouse stage on warmer so it can retain heat and remain warm once laser procedure begins.

2. Mouse Anesthesia and Pre-laser Preparation

- Before injecting anesthesia, inspect the eye macroscopically to ensure it has no deformities or abnormalities that diminish corneal clarity (e.g. cataract).
- Weigh mouse.
- Record weight, sex, and animal ID number.
- Using weight, calculate appropriate amount of anesthetic to be used based on guidelines given by institution (e.g. 100 mg/kg ketamine hydrochloride, 10 mg/kg xylazine OR tribromoethanol 250 mg/kg; for a 20 g mouse inject 0.20 ml xylazine/ketamine cocktail OR 0.25 ml of tribromoethanol). Have a table of pre-calculated dosages per weight in increments of 1 g in order to reduce mathematical errors.
- Scruff mouse and inject anesthetic intraperitoneally based on calculations in step 2.4.
- Place mouse on animal warmer and wait until mouse is completely anesthetized by checking the pedal reflex via toe pinch (approximately 3-5 min).
- Roll up a tissue wipe and protect the mouse's nasal area to prevent aspiration of liquid roll-off. Roll mouse on its side and place a drop (approximately 30 μ l) of tetracaine hydrochloride into each eye for topical anesthesia. Wait 2 min for solution to take effect.
- Repeat step 2.7 with one drop of topical Tropicamide for pupillary dilation. Alternatively, use phenylephrine hydrochloride (2.5%) for dilation.
- Wait 2 min for solutions to take effect; keep animal on warmer during this time.
- After appropriate time has elapsed, quickly place the mouse on the mouse stage and place the stage on chin rest of slit lamp.
- Turn on slit lamp to the lowest light brightness and check the degree of pupillary dilation. If pupil is not adequately dilated (approximately 2.5-3 mm), return mouse to animal warmer and wait. Alternatively, administer another drop of Tropicamide. Once eye is sufficiently dilated, proceed to laser procedure.

3. Laser Procedure

Note: Ensure other persons in the room wear protective goggles when away from laser-protected slit lamp eye-piece

1. Adjust the placement of mouse on the mouse-stage, so that it is ideally positioned for visualization of optic nerve (see 3.1.2).
 1. Orient the mouse on its holder so it lies horizontally, perpendicular to slit lamp beam, with the head at one side and tail at the other. Ideal mouse placement will make optic nerve visualization much easier once cover slip is applied.
 2. Slightly turn the mouse so it is at a $\sim 170^\circ$ angle with the head closer to laser operator.
 3. Ensure that mouse is as close as possible to slit lamp, yet still in a position where it is stable and where the operator's hand will have enough space for fine manipulation.
2. After the mouse is ideally positioned, place one drop of artificial tear solution on a 25 mm x 25 mm glass coverslip.
 1. Place one drop of artificial tear solution on mouse's opposite eye – this will ensure eye is hydrated and help delay cataract formation.
3. Hold corner of coverslip between thumb and pointer fingers; position so that the glass is squeezed between tips of both fingers.
4. Gently wrap the remaining three fingers around the animal's body for support and hand stabilization. Position hand so that the glass coverslip can be easily placed on the mouse's eye.
 1. Be sure that the wrist is stabilized on a firm surface in order to reduce hand tremor.
5. Once stable position is obtained, carefully press glass coverslip (with drop of artificial tear still adhered) onto the mouse's eye.
 1. Make sure the coverslip is positioned as perpendicular as possible to the laser beam in order to prevent laser beam scatter or reflection. The coverslip acts as a contact lens to flatten the cornea.
6. Look through slit lamp and with free hand toggle focus until retina can be visualized. The retina will have a light-yellow/red color depending on the location visualized, distinct, red vessels will be visible.
7. Slowly and carefully manipulate mouse head and/or coverslip until visualizing the optic nerve. The optic nerve will be yellow in color with multiple vessels radiating from it.
8. Once operator has confirmed visualization of optic nerve, turn on laser focusing beam.
9. Once laser beam has been turned on, maneuver laser focusing beam to desired position (approximately 1 disc diameter from the optic nerve).
10. Focus laser beam on the RPE of the eye fundus. Proper focus is achieved by having the sharpest and clearest laser beam. If aiming beam looks oval or out of focus, toggle slit lamp focus or re-position glass coverslip.
11. Once the aiming beam is focused on RPE, initiate laser administration using the laser's foot trigger.
 1. Be sure to avoid retinal vessels to prevent intraocular hemorrhage.
12. Watch for the appearance of a bubble immediately after laser administration. The outline of the laser shot should be clear and not hazy in any way.
 1. If the laser shot does not result in bubble formation, or area of impact looks hazy (cloudy appearance with ill-defined circular border vs. clear, sharply defined border of a successful impact), or if hemorrhage is seen after laser administration, do NOT include these lesions for future analysis.
13. Repeat steps 3.10-3.12 for all desired CNV positions (usually at 3, 6, 9, and 12 o'clock positions around optic nerve). If laser inductions are applied at approximately same distance from optic nerve, refocus should not be necessary. However, due to the strong curvature of the mouse eye and small variations that may exist in the retina, refocusing the beam may be necessary between consecutive laser administrations.
14. Record in a notebook the location and result of each laser shot administration and result (successful, hazy, hemorrhage, etc.) of each administered shot for the eye. Be sure to place the laser in stand-by mode when not in use.
15. Repeat 3.1-3.14 for the mouse's other eye, if needed, using the opposite hand for stabilization and a new coverslip.
16. After all desired laser shots are administered, turn off laser and slit-lamp.
17. Discard coverslip and place mouse on warmer for recovery from anesthesia. Macroscopically inspect eye for any injury and place a drop of artificial tear solution to keep the eye hydrated and potentially prevent future cataract development. Once mouse recovers from anesthesia, return to cage.

	AVERTIN	AVERTIN	AVERTIN	XYL/KET	XYL/KET
Mouse Weight (g)	Dose (mg/kg)	Solution Concentration (mg/ml)	Anesthetic Dose (ml)	Dose (mg/kg)	Anesthetic Dose (ml)
15	250	20	0.1875	100 mg/kg ketamine; 10 mg/kg xylazine	0.15
16	250	20	0.2	100 mg/kg ketamine; 10 mg/kg xylazine	0.16
17	250	20	0.2125	100 mg/kg ketamine; 10 mg/kg xylazine	0.17
18	250	20	0.225	100 mg/kg ketamine; 10 mg/kg xylazine	0.18
19	250	20	0.2375	100 mg/kg ketamine; 10 mg/kg xylazine	0.19
20	250	20	0.25	100 mg/kg ketamine; 10 mg/kg xylazine	0.2
21	250	20	0.2625	100 mg/kg ketamine; 10 mg/kg xylazine	0.21
22	250	20	0.275	100 mg/kg ketamine; 10 mg/kg xylazine	0.22
23	250	20	0.2875	100 mg/kg ketamine; 10 mg/kg xylazine	0.23
24	250	20	0.3	100 mg/kg ketamine; 10 mg/kg xylazine	0.24
25	250	20	0.3125	100 mg/kg ketamine; 10 mg/kg xylazine	0.25
26	250	20	0.325	100 mg/kg ketamine; 10 mg/kg xylazine	0.26
27	250	20	0.3375	100 mg/kg ketamine; 10 mg/kg xylazine	0.27
28	250	20	0.35	100 mg/kg ketamine; 10 mg/kg xylazine	0.28
29	250	20	0.3625	100 mg/kg ketamine; 10 mg/kg xylazine	0.29
30	250	20	0.375	100 mg/kg ketamine; 10 mg/kg xylazine	0.3

Table 1: XylKet Dosage Chart.

Representative Results

Quantification of CNV lesions can be performed through analysis of flat-mounted choroids using immunofluorescence staining to label the CNV vessels. The two most frequently employed methods of tissue preparation are FITC-dextran labeling, done via perfusion immediately before animal sacrifice, or post-mortem immuno-staining with an endothelial cell marker. Both of these methods have been described previously in detail^{13,14,21}; **Figures 1** and **2** show examples of each, respectively. After confocal microscopy image acquisition, either area (2-Dimensions) or volume (3-Dimensions) can be calculated and visualized with ImageJ software or Volocity. In addition to quantification, OCT imaging can be used to visualize the CNV lesion *in vivo*. An example of a cross sectional image of the retina with resultant CNV is shown in **Figure 3**.

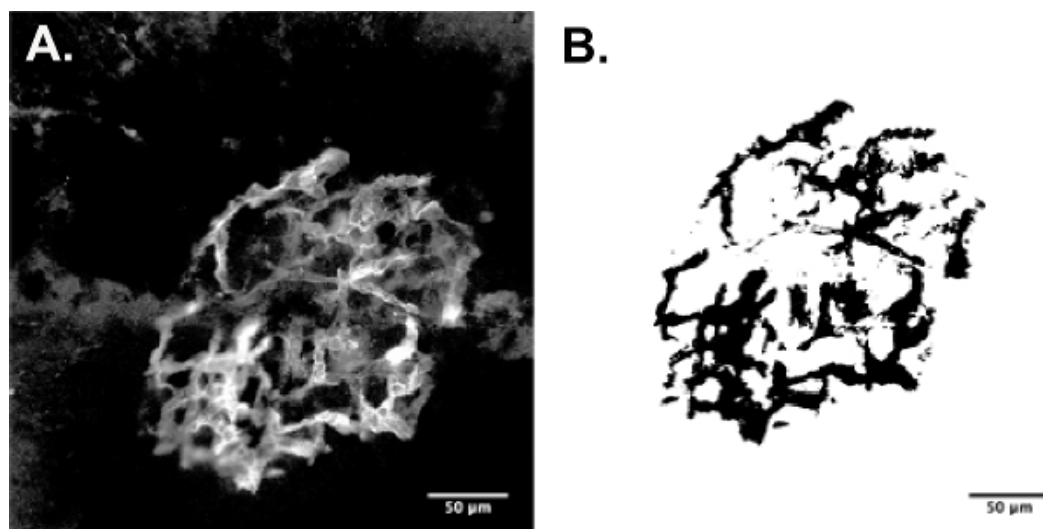


Figure 1: CNV Perfusion Staining & Area (2D) Calculation Example (25X). (A) FITC dextran perfused CNV lesion. (B) ImageJ area quantification method via thresholding. Mouse Strain: C57BL/6J. [Please click here to view a larger version of this figure.](#)

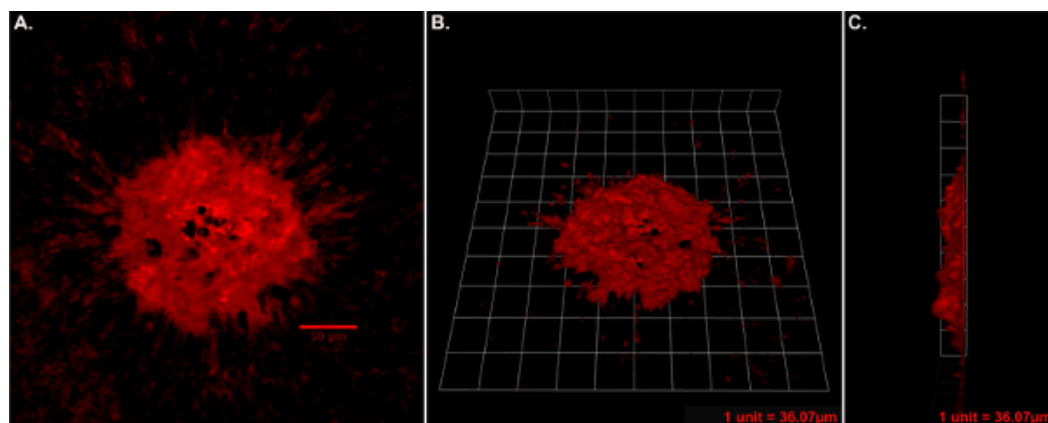


Figure 2: CNV Immunostaining & Volume (3D) Calculation Example (25X). (A) Isolectin GS-IB4 stained CNV lesion. (B) 3D reconstruction of CNV lesion *en face* view. (C) 3D reconstruction side view (B and C one tile width = 35 μm). Mouse Strain: C57BL/6J. [Please click here to view a larger version of this figure.](#)

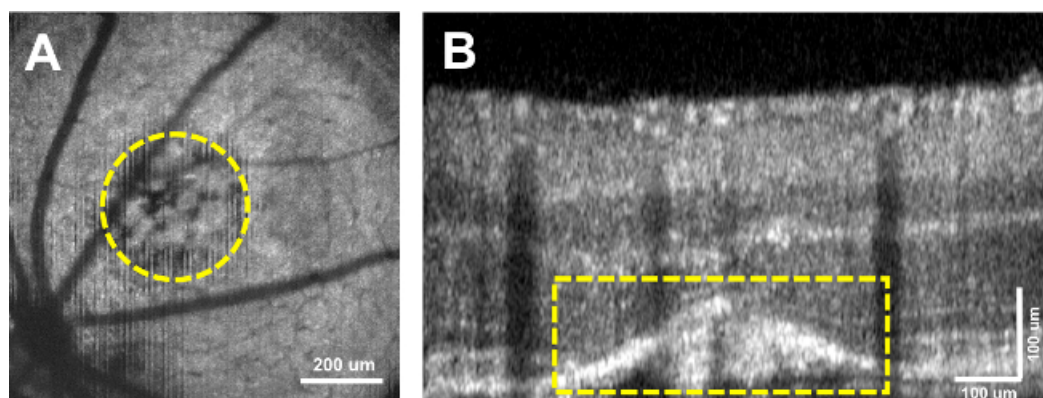


Figure 3: OCT Cross-Sectional CNV Visualization. (A) OCT en face view of CNV lesion. (B) OCT cross-sectional B-scan of retina with CNV circled in yellow. Mouse Strain: C57BL/6J. [Please click here to view a larger version of this figure.](#)

Discussion

There are multiple factors that can affect laser delivery and resultant CNV lesion development after successful laser-induction. These factors should be controlled for and standardized in order to have the most reliable results. The most pertinent of these factors are mouse selection (genotype, age, and sex), anesthetic selection, and laser settings.

The specific mouse model used can have a significant effect on the course of CNV development. The most widely used genotype is the C57BL/6 mouse. The vendor from which the animals are obtained can affect the resultant CNV size. Poor et al. demonstrated significant differences in final CNV lesion size in C57BL/6 mice from Jackson, Charles Rivers, and Taconic laboratories, with mice from Taconic developing significantly larger CNV than the other two vendors⁴. Therefore, purchasing from one company and using all mice from that same vendor will help to minimize external differences in CNV lesion size. Age and sex of the mouse has also been shown to be an important factor to consider when designing the experiment. Female mice develop more CNV than male mice of the same age, and older mice of both sexes develop more CNV than younger mice^{22,23}. Depending on the experimental parameters, operators should keep these factors in mind. For example, if operators are using the laser-CNV procedure to elucidate mechanistic and drug-development purposes, both sexes at different ages should be used to define mechanisms that are specific to the sexes and those that are not.

Proper anesthesia is a critical step for this procedure, especially during the learning process. Most IACUC approved regimens can induce anesthesia for at least 15-30 min, which is more than enough time to deliver 4-5 laser shots to each eye once the procedure has been mastered. However, if too much time elapses, anesthesia can lead to reversible lens opacification, rendering the eye optically impervious for experimental CNV²⁴. The two main protocols used to induce anesthesia are a xylazine/ketamine cocktail or tribromoethanol (TBE) delivered intraperitoneally. Although some reports posit the advantages of TBE to xylazine/ketamine in terms of cataract formation, both eventually result in the development of a cloudy lens if the operator does not work quickly¹⁴. One way to extend the time before cataract development is to maintain hydration of the eye, as mentioned in the detailed protocol, through application of artificial tears²⁵. This method, regardless of anesthetic substance used, should help delay cataract formation and give the operator more time to complete the procedure.

Laser settings can be a major factor in the reliable induction of CNV. Calibrating the laser power and duration are an important preliminary step before conducting the procedure on experimental animals. Laser shots that cause hemorrhage or are out of focus without bubble formation should be excluded from calculation, as this disrupts the CNV development process. If multiple vessels are ruptured causing diffuse hemorrhage, the entire eye should be excluded. Ideally, the lowest power and shortest duration of laser that consistently ruptures Bruch's membrane causing bubble formation and a lesion with clear demarcation should be used⁴. Protocols experimenting with different power settings have demonstrated that increased power and duration lead to excessive tissue damage and subsequently lower rates of CNV formation^{4, 14, 17}. Furthermore, location of the laser injury can also affect CNV development. Impacts delivered approximately 1 disc diameter (DD) from the optic disk yielded significantly larger area CNV volumes than those delivered <1 DD or 2 or more DDs away²³. Depending on the post-laser analysis, lesion location may or may not be crucial. For example, if an OCT image is to be obtained of all lesions, central location around the optic nerve is vital. Contrastingly, if lesions are to be analyzed via flat mount, lesion location is not as crucial. Finally, ensure that last shots are not placed too close to one another or else two lesions may "grow" together.

The CNV assay is a robust method to experimentally study neovascular AMD. The angiogenesis resulting from laser induction is similar in location and overall appearance to the angiogenesis observed in human AMD patients. However, it is far from a perfect model. Unlike the human eye, mice do not have a defined macula, and the acute injury-related angiogenesis seen in the laser-induced CNV model fundamentally differs from the genetically influenced, chronic pathology of AMD^{7,8,14}. The mouse retinal environment is healthy and the resultant angiogenesis occurs as a reaction to the trauma caused by the laser impact, rather than genetic/environmental factors and age, as in human AMD. Contrastingly, the human retinal environment in AMD is in a state of chronic inflammation, during which abnormalities in VEGF expression and other cytokines cause CNV³. Clearly, the neovascular development in these two environments is markedly different.

In conclusion, the laser-induced CNV protocol is one that is initially difficult to perform but ultimately rewarding to master. The fine dexterity needed to hold the mouse and coverslip, as well as manipulate the coverslip and mouse head to visualize the optic nerve are exercises that require patience and practice, especially since they need to be performed well using either hands of the operator. However, once the technique is learned it can be an efficient way to implement experimental CNV and can be applied to most aspects of neovascular AMD research.

Disclosures

The authors declare they have no competing financial interests.

Acknowledgements

The authors would like to acknowledge Jonathan Chou, MD for his assistance on preparation and editing of the final manuscript and Wenzhong Liu for the OCT data. We would also like to acknowledge support from the Macula Society Research Grant (AAF), support from an unrestricted grant to Northwestern University from Research to Prevent Blindness, Inc., New York, NY, USA, and support from NIH-EY019951.

References

1. Bressler, N. M., Bressler, S. B., & Fine, S. L. Age-related macular degeneration. *Surv Ophthalmol.* **32**, 375-413 (1988).
2. Congdon, N. et al. Causes and Prevalence of Visual Impairment Among Adults in the United States. *Arch Ophthalmol.* **122**, 477-485, (2004).
3. Jager, R. D., Mieler, W. F., & Miller, J. W. Age-Related Macular Degeneration. *NEJM.* **358**, 2606-2617, (2008).
4. Poor, S. H. et al. Reliability of the Mouse Model of Choroidal Neovascularization Induced by Laser Photocoagulation. *IOVS.* **55**, 6525-6534, (2014).
5. Ryan, S. J. The development of an experimental model of subretinal neovascularization in disciform macular degeneration. *Trans Am Ophthalmol Soc.* **77**, 707-745 (1979).
6. Miller, H., Miller, B., Ishibashi, T., & Ryan, S. J. Pathogenesis of laser-induced choroidal subretinal neovascularization. *IOVS.* **31**, 899-908 (1990).
7. Pennesi, M. E., Neuringer, M., & Courtney, R. J. Animal models of age related macular degeneration. *Molr Aspects Med.* **33**, 487-509 (2012).

8. Grossniklaus, H. E., Kang, S. J., & Berglin, L. Animal Models of Choroidal and Retinal Neovascularization. *Prog Retin Eye Res.* **29**, 500-519, (2010).
9. Zeiss, C. J. REVIEW PAPER: Animals as Models of Age-Related Macular Degeneration: An Imperfect Measure of the Truth. *Vet Pathol Online.* **47**, 396-413, (2010).
10. Tobe, T. *et al.* Targeted Disruption of the FGF2 Gene Does Not Prevent Choroidal Neovascularization in a Murine Model. *Am J Pathol.* **153**, 1641-1646 (1998).
11. He, L., & Marneros, A. G. Macrophages Are Essential for the Early Wound Healing Response and the Formation of a Fibrovascular Scar. *Am J Pathol.* **182**, 2407-2417 (2013).
12. Hoerster, R. *et al.* In-vivo and ex-vivo characterization of laser-induced choroidal neovascularization variability in mice. *Graefes Arch Clin Exp Ophthalmol.* **250**, 1579-1586, (2012).
13. Jawad, S. *et al.* The Role of Macrophage Class A Scavenger Receptors in a Laser-Induced Murine Choroidal Neovascularization Model. *IOVS.* **54**, 5959-5970, (2013).
14. Lambert, V. *et al.* Laser-induced choroidal neovascularization model to study age-related macular degeneration in mice. *Nat. Protocols.* **8**, 2197-2211, (2013).
15. Sakurai, E., Anand, A., Ambati, B. K., van Rooijen, N., & Ambati, J. Macrophage Depletion Inhibits Experimental Choroidal Neovascularization. *IOVS.* **44**, 3578-3585, (2003).
16. Espinosa-Heidmann, D. G. *et al.* Macrophage Depletion Diminishes Lesion Size and Severity in Experimental Choroidal Neovascularization. *IOVS.* **44**, 3586-3592, (2003).
17. Giani, A. *et al.* In Vivo Evaluation of Laser-Induced Choroidal Neovascularization Using Spectral-Domain Optical Coherence Tomography. *IOVS.* **52**, 3880-3887, (2011).
18. Kwak, N., Okamoto, N., Wood, J. M., & Campochiaro, P. A. VEGF Is Major Stimulator in Model of Choroidal Neovascularization. *IOVS.* **41**, 3158-3164 (2000).
19. Reich, S. J. *et al.* Small interfering RNA (siRNA) targeting VEGF effectively inhibits ocular neovascularization in a mouse model. *Molr Vis.* **9**, 210-216 (2003).
20. Baffi, J., Byrnes, G., Chan, C. C., & Csaky, K. G. Choroidal Neovascularization in the Rat Induced by Adenovirus Mediated Expression of Vascular Endothelial Growth Factor. *IOVS.* **41**, 3582-3589 (2000).
21. Claybon, A., & Bishop, A. J. R. Dissection of a Mouse Eye for a Whole Mount of the Retinal Pigment Epithelium. *JoVE.* 2563, (2011).
22. Espinosa-Heidmann, D. G. *et al.* Age as an Independent Risk Factor for Severity of Experimental Choroidal Neovascularization. *IOVS.* **43**, 1567-1573 (2002).
23. Zhu, Y. *et al.* Improvement and Optimization of Standards for a Preclinical Animal Test Model of Laser Induced Choroidal Neovascularization. *PLoS ONE.* **9**, e94743, (2014).
24. Weinstock, M., & Stewart, H. C. Occurrence in rodents of reversible drug-induced opacities of the lens. *British J Ophthalmol.* **45**, 408-414 (1961).
25. Ridder III, W. H., Nusinowitz, S., & Heckenlively, J. R. Causes of Cataract Development in Anesthetized Mice. *Exp Eye Res.* **75**, 365-370 (2002).